DISCLAIMER

This report was prepared as an account of work sponsored by an agency of the United States Government. Neither the United States Government nor any agency thereof, nor any of their employees, makes any warranty, express or implied, or assumes any legal liability or responsibility for the accuracy, completeness, or usefulness of any information, apparatus, product, or process disclosed, or represents that its use would not infringe privately owned rights. Reference herein to any specific commercial product, process, or service by trade name, trademark, manufacturer, or otherwise does not necessarily constitute or imply its endorsement, recommendation, or favoring by the United States Government or any agency thereof. The views and opinions of authors expressed herein do not necessarily state or reflect those of the United States Government or any agency thereof. Reference herein to any social initiative (including but not limited to Diversity, Equity, and Inclusion (DEI); Community Benefits Plans (CBP); Justice 40; etc.) is made by the Author independent of any current requirement by the United States Government and does not constitute or imply endorsement, recommendation, or support by the United States Government or any agency thereof.

LA-UR-25-30636

Approved for public release; distribution is unlimited.

Title:	MONITORING THE STRUCTURAL HEALTH OF THE STAGE-FOUR GIBBS RESISTOR In Order to Maintain a Functioning Pulse-Forming Network
Author(s):	Rogers, Cayman Abriina
Intended for:	Report
Issued:	2025-10-27

MONITORING THE STRUCTURAL HEALTH OF THE STAGE-FOUR GIBBS RESISTOR

In Order to Maintain a Functioning Pulse-Forming Network

University of California – San Diego
Spring Quarter, 2025

Rogers, Cayman Abriina
c1rogers@ucsd.edu

1 Table of Contents

2 Table of Figures

3 Table of Equations

4 Problem Definition

The Dual-Axis Radiographic Hydrodynamic Test (DARHT) facility at Los Alamos National Laboratory (LANL) is a critical facility used for nuclear weapons research and development (Los Alamos National Laboratory). Its primary function is to provide high-resolution, real-time images of the behavior of materials under extreme conditions, specifically during the hydrodynamic testing of nuclear weapons surrogates. The facility uses advanced radiographic techniques, such as dual-axis X-ray imaging, to capture detailed snapshots of these materials as they react to high-pressure environments.

DARHT plays a key role in maintaining the safety, security, and reliability of the U.S. nuclear arsenal, supporting the Stockpile Stewardship Program. The facility helps ensure that nuclear weapons perform as designed without the need for nuclear tests. Its dual-axis radiography provides more precise data than traditional single-axis imaging, offering a comprehensive view of the internal dynamics of a weapon's primary stage.

FIGURE 1: THE DUAL-AXIS RADIOGRAPHIC HYDRODYNAMIC TEST FACILITY (DARHT) AT TA-15. PHOTO COURTESY LANL (LOS ALAMOS REPORTER)

DARHT is a linear induction accelerator. The second Axis, referred to as Axis II, consists of 74 induction cells and drivers which provide a total acceleration of 20 MeV to a 2kA electron beam. The cell drivers are pulse-forming networks (PFNs) which are tuned to provide a set voltage regulation. These PFNs are designed using a complex assembly of resistors, capacitors, and inductors. One of the resistor components, the Gibbs resistor, is integrated into the design to set the overall output impedance of the PFN, as well as adjust the rise time of the pulse shape created by the PFN. There are four stages of Gibbs resistors built into DARHT's PFNs. The

Gibbs resistors built into the final stage of these PFNs, the fourth stage, are prone to blow out during use.

When a Gibbs resistor breaks, the only way to know for certain is to pull the PFN out from its tank at DARHT and take it in for maintenance. The oil must be drained out of the PFN chassis before the MARX stages can be pulled out and inspected. The only way to check that a Gibbs resistor has busted is through visual inspection. The argument made in the following sections is for the use of a diagnostic already integrated into DARHT's system in monitoring and diagnosing the structural health of the fourth-stage Gibbs resistor. This diagnostic, a Rogowski coil, provides information on the output current of the PFN. As the absence or breakdown of the fourth-stage Gibbs resistor alters the output impedance of the PFN, then the current output should also be altered. The Rogowski coil will be used to monitor this fluctuation in the output current when a Gibbs resistor has failed or when it is in the process of failing.

5 Background Information

DARHT Axis II is a linear induction accelerator consisting of 74 cells (as seen in Figure 2). These cells drive the electron beam forward, accelerating the particles until they hit a target, producing X-rays for imaging purposes (Waldron and Reginato). The induction cells are driven by type-E pulse-forming networks. A Pulse-Forming Network (PFN) is an electrical circuit used to generate a high-energy, shaped electrical pulse, often used in applications that require a precise pulse waveform (Cook and Hotta 39-58). The main purpose of a PFN is to convert a continuous DC (direct current) voltage into a short-duration, high-amplitude pulse. Typically, a PFN consists of a series of capacitors, inductors, resistors, and switches. The capacitors store energy, while the inductors and resistors help shape and control the pulse's characteristics, such as its duration and rise time. The PFN discharges its stored energy through a load when the switch is triggered, creating a pulse with a specific rise time, duration, and amplitude.

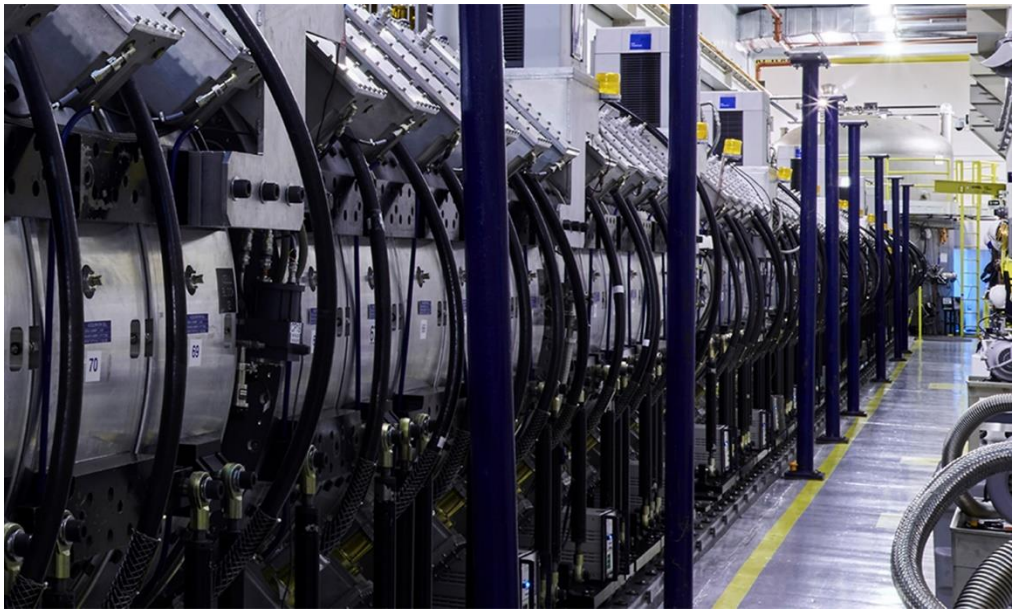

FIGURE 2: AXIS II ACCELERATOR HALL (JILL GIBSON)

A Type-E Pulse-Forming Network is a more specialized and optimized version of a PFN, designed for applications where specific pulse characteristics are required; these pulse characteristics being sharp rise times, precise pulse duration, and accurate timing (*General Atomics*). Type-E PFNs often employ more complex circuit configurations to achieve these advanced characteristics. Unlike standard PFNs, Type-E PFNs may use hybrid designs, such as transmission-line techniques or resonant circuits, where the components are arranged to provide better control over pulse shape, rise time, and decay. These networks are typically designed to handle higher voltages and energies more efficiently, making them suitable for more demanding applications.

The key design differences between a standard PFN and a Type-E PFN lie in the specifics of pulse shaping, load matching, and impedance control. While standard PFNs are effective for generating basic pulse shapes, Type-E PFNs focus on achieving a highly controlled, well-defined pulse with specific parameters, such as sharp rise times and precise timing. Type-E PFNs are also optimized for impedance matching between the network and the load, ensuring that the pulse is delivered efficiently without reflections or energy loss. This is particularly important in the DARHT accelerator system.

A Guillemin Type E network (the PFN used at DARHT) consists of a network where the capacitance in each mesh (an electrical circuit that is an independent loop that does not enclose other loops within it), is the same, and there is mutual inductance between adjacent coils (see Figure 3). The squareness of the output pulse depends on the number of meshes. The rise time of the pulse is determined by the rise time of the first mesh in the network, which is the one closest to the load. The pulse width is twice the one-way transit time of the wave (i.e. a smooth, flat-top pulse). If the characteristic impedance of the PFN matches that of the load, the energy will be nearly fully absorbed by the load (with no reflection), and the voltage across the load will be half the charge voltage of the PFN capacitors. Typically, the inductor closest to the load is made larger than the others to prevent overshoot, and this inductor is about 30% larger than the others.

At DARHT, Guillemin Type E networks are used to deliver a precise, high-voltage pulse to accelerator cells. It is crucial for this pulse to be flat; if it is not, then there will be an energy delta on the beam. If this occurs, then focus of the beam will not be ideal, leading to a larger x-ray spot. Therefore, the radiographic image provided by DARHT will have a lower resolution than if the pulse had been flatter. Thus, achieving a flat pulse shape is fundamental for effective and reliable operation of DARHT.

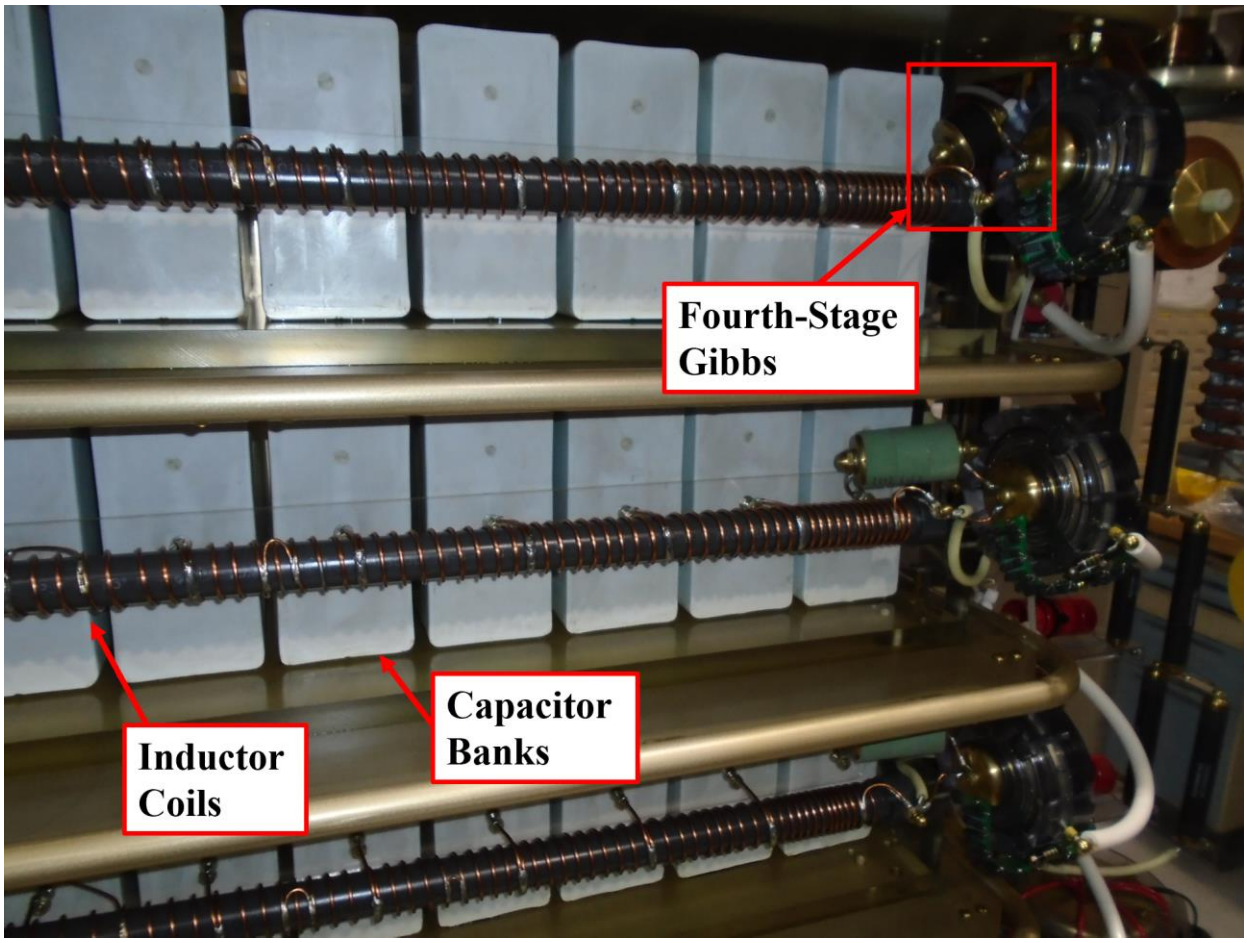

FIGURE 3: INTERNAL VIEW OF THE DARHT PFN

The DARHT PFNs consists of four MARX stages (Waldron and Reginato). A MARX circuit is an electrical circuit used to generate high-voltage pulses by charging capacitors in parallel and then discharging them in series. Inductors are integrated into the circuit to limit the rate of current change when the capacitors discharge into the load, which helps control the rise time of the pulse and ensures the pulse has the desired characteristics. Thus, when a capacitor discharges, the current must first travel through the inductor before entering the spark-gap switch. As stated in the previous paragraph, the capacitor closest to the load discharges through an inductor made larger than the others. However, in the DARHT PFNs, in lieu of utilizing a final inductor, the current must instead travel through a Gibbs resistor (see Figure 3). The Gibbs resistor is used to adjust the rise time and front corner of the pulse. It is the signal that, once added to each frequency produced by the accompanying capacitors, acts as the peaking shoulder to give the square wave sharp edges. If the Gibbs' resistance is too high, the pulse will undershoot and look more like a mound. If the resistance is too low, the pulse will be too sharp and there will be excess ringing sent out through the signal.

6 Proposed System

Built into the DARHT PFNs are four MARX stages; ergo, there are four Gibbs resistors. The individual resistance of each resistor is set so that the output impedance of the pulse is 20Ω. The Gibbs resistor built into the fourth stage has a resistance of 2Ω. After a certain number of shots, this resistor will fail. Currently, the only way to detect precise failure mechanism is to visually inspect the MARX stages, a lengthy process which requires the dismantling of the PFN. The proposed solution suggests using the Rogowski coil centered around the output cables to monitor disturbances in current caused by breakdown of the fourth-stage Gibbs resistor.

A Rogowski coil is a type of electrical sensor used to measure alternating current (AC) and high-frequency currents (*PEM UK*). It consists of a helical coil of wire, typically wound around a non-magnetic core, that is placed around a conductor through which the current is flowing. Unlike traditional current transformers, the Rogowski coil does not require a magnetic core but instead relies on the principle of electromagnetic induction to measure the current (an example is shown in Figure 4).

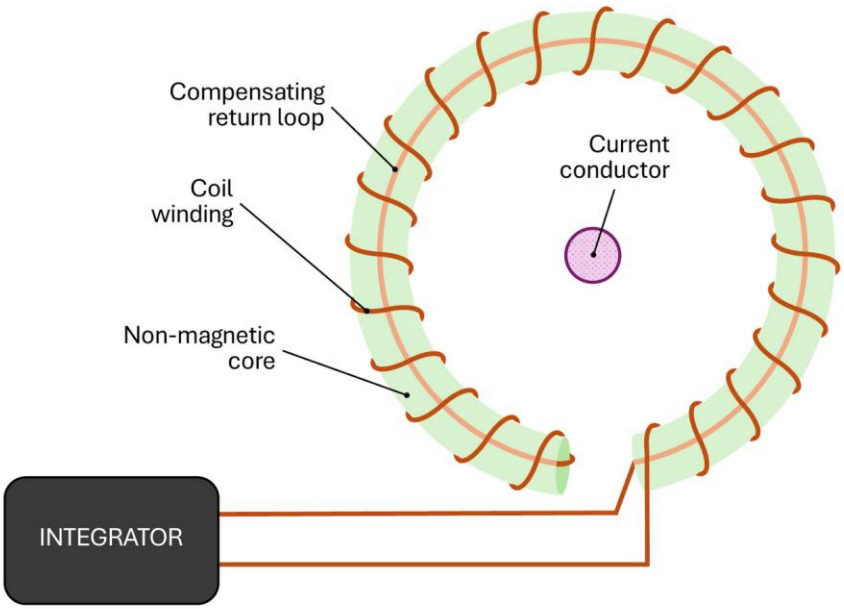

FIGURE 4: THE ROGOWSKI COIL, INTRODUCED IN 1912 BY W. ROGOWSKI AND W. STEINHAUS, IS A CORELESS, FLEXIBLE, NON-SATURATING, AIR-WOUND COIL USED FOR MEASURING ALTERNATING CURRENT (*PEM UK*)

The operation of a Rogowski coil is based on Faraday's law of induction, which states that a time-varying magnetic field will induce a voltage in a conductor. As the current in the conductor generates a magnetic field that changes over time, this varying magnetic field passes through the Rogowski coil. According to Faraday's law, the rate of change of this magnetic field induces a voltage in the coil, which is proportional to the derivative of the current. The voltage generated

by the Rogowski coil is thus a measure of the rate of change of the current, and to obtain the actual current, this voltage signal is integrated electronically.

One of the advantages of a Rogowski coil is its ability to measure high currents with high accuracy while maintaining a linear response over a wide range of current levels. Since it does not require a magnetic core, the Rogowski coil can be made lightweight, flexible, and easily adapted to large conductors or complex geometries. Additionally, the absence of a core means there are no saturation effects, allowing it to handle high currents without distortion.

When a Gibbs resistor breaks, the signal sent out by the final capacitor in the MARX series will be met with a resistance much higher than 2Ω. It will be met with what is essentially an infinite resistance. However, once enough voltage has built up on one side of the busted resistor the current will arc across the oil gap, bringing the resistance down to 0Ω. It is not known when this breakdown occurs; however, the current readout provided by the Rogowski coil can provide a threshold for knowing when the Gibbs' resistance is approaching infinity, or when it is equal to zero. If the resistance is too low, then the current readout will dip down; if the resistance is too high, then the current readout will spike and there will be more ringing in the signal.

If one of the Gibbs resistors is actively failing, then the resistance will increase (details explained below). There will be no oil gap involved in this scenario; thus, the current waveforms will continue to drop as the resistor grows less and less efficient. Monitoring these decaying waveforms in real-time is useful because the Gibbs resistor can be caught at fault before it completely fails.

7 Operational Evaluation and Environmental Effects

7.1 Definition of Damage

The Gibbs resistors are considered damaged if their resistivity increases. The resistivity of the ceramic material used to create the Gibbs resistors is lower than that of oil. As the Gibbs resistors are submerged in oil during use of the PFNs, oil will be the working environment. It is theorized that as the resistors crack and fracture with time, then oil fills in the gaps of the cracks and is now taking up the volume of space where the material of the resistors was once evenly distributed. The oil will also fill in space along the exterior surface of the resistor where the ceramic may have chipped off. This increases the resistivity of the gap between the final capacitor and the air gap switch and thus increases the resistance of the Gibbs component. One can see this alteration to the resistance in viewing the following formula:

$$\boldsymbol{R = \frac{\rho L}{A}}$$

EQUATION 1

Where R is the resistance of the material, ρ is the resistivity of the material, L is the length of the resistor, and A is the cross-sectional area of the resistor. Although A will increase slightly as cracks in the resistor form, so too shall L. Ergo, one may ignore the increase in diameter of the resistor in the denominator, as these effects will be counteracted by the elongation of the resistor

due to cracks. The resistivity of the Gibbs resistors is $0.0104\Omega m$, while the resistivity of mineral oil is about $10^{13}\Omega m$. One can see that as the oil fills in the gaps, the Gibbs resistor's *R*-value will increase.

Similarly, if the Gibbs resistor completely fails and all ceramic material breaks away from the mesh, then the resistivity of the gap between the final capacitor and the air gap switch will increase. This resistivity will equate to that of only oil, allowing for the current to encounter what is essentially an infinite resistance. Both scenarios, one in which the resistor is fractured, the other when it is completely damaged and is no longer a part of the circuit, are defined as damage to the Gibbs resistor.

7.2 Justification – Economic Loss

Monitoring the structural health of the Gibbs resistors is beneficial for a number of reasons. If one can monitor the waveforms and watch the Gibbs resistor progressively deteriorate, then the PFN can be decommissioned before catastrophic failure or damage to other components occurs. The Gibbs resistor can then be replaced prior to failure. This is the ideal scenario because when a Gibbs resistor bursts and the damage is not made known to the operators, then they will continue to fire the PFN with an oil gap in lieu of a resistor. The oil gap created by the absence of the resistor acts as a poorly designed spark gap. Charge will build up on the capacitor side until the current eventually arcs toward the switch. In the past, firing in this configuration has blown circuit boards built into the top of the PFN. It also has the potential to damage other elements of the PFN because the output impedance of the signal no longer matches the load. If the output impedance does not match that of the load, then the signal reflected back into the PFN post-firing will be large enough to break circuit elements. Also, if the Gibbs resistor is allowed to explode, then dust is distributed throughout PFN, creating HV breakdown paths at other locations.

It is best to catch the degradation of the fourth-stage Gibbs resistor prior to its complete failure because it will take up less man time to repair the PFN. Repairing PFNs is an arduous process, as they must be removed from their oil tanks at the accelerator, relocated to a refurbishing station, and diagnosed via visual inspection. While it is easy to spot the broken Gibbs resistor once a PFN is out of its tank, the state of the resistor cannot be known until the PFN is removed from the tank. Furthermore, if the decommissioned PFN was run *after* the resistor broke, then the technicians refurbishing the PFN must check that all other circuit components are running smoothly, as the healthy state of these circuit components can no longer be presumed.

7.3 Environmental and Operational Variability

There is little variability in the environment the Gibbs resistors are built into. According to the manufacturer, the tolerance of each individual 2Ω resistor is 0.2Ω (*HVR Advanced Power Components*). Additionally, the resistivity of the oil may vary, depending on its age. The oil in each tank is not flushed out periodically, but rather on a failure-by-failure basis (i.e. if a PFN is being refurbished, the oil tank will be drained and refilled; else, there is no procedure to periodically change out the oil that submerges the PFNs).

However, there is a large variation in the usage of the PFNs. The PFNs undergo an assortment of stresses depending on how frequently the accelerator is being used and the amount of charge

each PFN must hold for each shot. For example: there may be one year when DARHT is called to enact one or two hydro shots. In other years, it may have to fire hydro shots once a month. Each hydro shot is accompanied by runup shots, used to tune the beam and check for irregularities in the procured images prior to shot day. Therefore, some Gibbs resistors undergo heavy loads at a high frequency, while others may undergo heavy loads at a light frequency. Vice versa, a PFN may undergo light loads at a heavy frequency, or heavy loads at a light frequency. The term "load" refers to the charge held by the PFN. A "light" load is considered to be a 31kV to 68kV pulsed-power shot; a "heavy" load is defined as a shot enacted at any charge set at the 68kV threshold or beyond. This means that not all Gibbs resistors will fracture or break down over the same time period. Some may deteriorate quickly, indicating a need for a set current threshold. Some Gibbs resistors will display a slow rise in resistance, while others may only approach infinite resistance for a few shots before bursting. Either way, if the dip in current can be spotted at the first signs of deterioration, then the operational frequency of the accelerator should not hinder the data.

8 Data Acquisition

Two sets of data were acquired for this study. The first was the comparative data collected at DARHT. Waveforms were retrieved from the data acquisition system that stores PFN signals after each shot. Each day the accelerator is run, current waveforms provided by the Rogowski coil are stored in the data acquisition system (DAAAC) and can be accessed for analysis at any time. Points of interest lay on the days when the fourth-stage Gibbs resistor burst. When a resistor bursts, the PFN is removed from DARHT and taken to a refurbishment station. Each PFN is numbered, and the days of PFN removal from DARHT are tracked in a logbook, with actions allocated to PFN numbers accordingly. The reasoning for removal is also logged. Therefore, using the PFN log information, current waveforms were pulled from the day of decommissioning. The shots preceding the PFN's removal provide insight into the state of the fourth-stage Gibbs resistor, as their current signals deviated from the standard readout.

While acquiring data from DARHT was not difficult, it was not the ideal data to use. A simulation was designed to model the pulse shape formed by the DARHT PFNs. It was run using varying values of resistance assigned to the fourth-stage Gibbs resistor. The simulation, used to observe current fluctuations in the circuit, was modeled using a different load than that of DARHT. The load at DARHT is an induction cell, a difficult load to model given the scope of the project. However, there is a test stand set up in the PFN refurbishment area that is used to test the reliability of the restored PFNs. This test stand has load circuitry that is simple to simulate: it is a resistive load with a constant resistance of 46.66 Ω. Therefore, the test stand was used to acquire data, as the waveforms provided by the output signal aligned with the model.

In choosing this approach, collecting data became more complex. Four tests were planned to be carried out to simulate the failure of a Gibbs resistor, though only three were performed. The first test was a baseline test, meaning data was collected on a PFN installed with a healthy, 2 Ω, Gibbs resistor. The data provided by this test served as the healthy standard of comparison for each succeeding test.

The next test involved the use of a 9Ω Gibbs resistor (as opposed to a healthy, 2Ω Gibbs resistor). Higher resistance was used to simulate the effect of an actively failing resistor. As a Gibbs resistor begins to break down, its resistance increases. Therefore, a 6Ω resistor was used to simulate the larger resistance induced by the breakdown of a Gibbs.

After the 6Ω resistor was tested, it was replaced by a copper wire. This placed the mesh in an "open circuit" configuration, essentially bringing the Gibbs resistance down to 0Ω. This was used to simulate the "oil gap" configuration taken on by the PFN when the Gibbs resistor breaks and all ceramic material falls away from the mesh. When a PFN is fired in this configuration, charge builds up on the capacitor-end of the gap, as it is met with what was essentially an "infinite resistance" at the gap, until it reaches a certain unknown voltage threshold. Once the voltage threshold is met, the current arcs across the oil gap, creating a closed loop in the mesh and shorting out the circuit. The shots taken using a shorting wire simulated this final stage of the shot.

The final test would have involved installing the resistor stack assembly while omitting the Gibbs resistor itself. This is the exact configuration taken on by the PFN when a Gibbs resistor fails. While this would have been the most telling test, in that it would not have simulated the failure of a Gibbs but instead provided direct information about a failed Gibbs, it was also the test that would have offered the highest likelihood of breaking other components inside the PFN. There are diode boards built into the PFN circuitry that are used to dampen the reflected signal returning to the load. If the Gibbs resistor is broken, then the output impedance of the PFN is lower, meaning the reflected load is larger than usual. The diode boards are built to receive a set voltage; therefore, if the voltage increases, some of the circuit elements built into the diode board will be damaged. As a result, only a limited number of shots could be taken in this configuration, the limiting factor being component damage. Unfortunately, data collection during this stage was forestalled, as time was a severely limiting factor during this experiment. This final test is planned to be enacted once enough spare PFNs are available for testing and proper time can be allocated to the test.

9 Features

As previously stated, the indicators of damage to the Gibbs resistors are cracks, chips, and any gaps formed between the disks forming the resistor stack. Any instance in which oil pools into space previously filled by the ceramic material of a resistor will lead to damage of the Gibbs resistor and, in turn, potentially other elements of the PFN. The feature that was monitored and measured over the course of the project was the PFN's output current, recorded by a Rogowski coil. An unusual spike or dip in this current is indicative of potential damage made to the fourth-stage Gibbs resistor. The current provided by the Rogowski coil can be monitored in real-time, meaning that an observer firing accelerator shots will have diagnostic readouts made available to them a few seconds after each shot is fired. A standard current waveform will reach expected current levels that correlate with charge voltage. For example, a beam-loaded shot fired at 31kV is expected to produce a pulse peak at just under 8kA. With each sequential shot, the current waveforms are expected to overlap one another. In other words: each PFN may produce a slightly different output current than its neighbor (a slight variance in accuracy), but it must

maintain a steady precision. If the current waveform begins to deviate from the PFN's established output current, then there may be a breakdown in one of the Gibbs resistors. This variance is the key indicator of a failing Gibbs resistor.

10 Simulations and Acquired Data

10.1 LTSpice Simulations and Acquired Data

Before any tests were performed, simulations of the circuit design incorporating a failing Gibbs resistor were run using LTSpice. The following is the layout of the DARHT PFN circuitry:

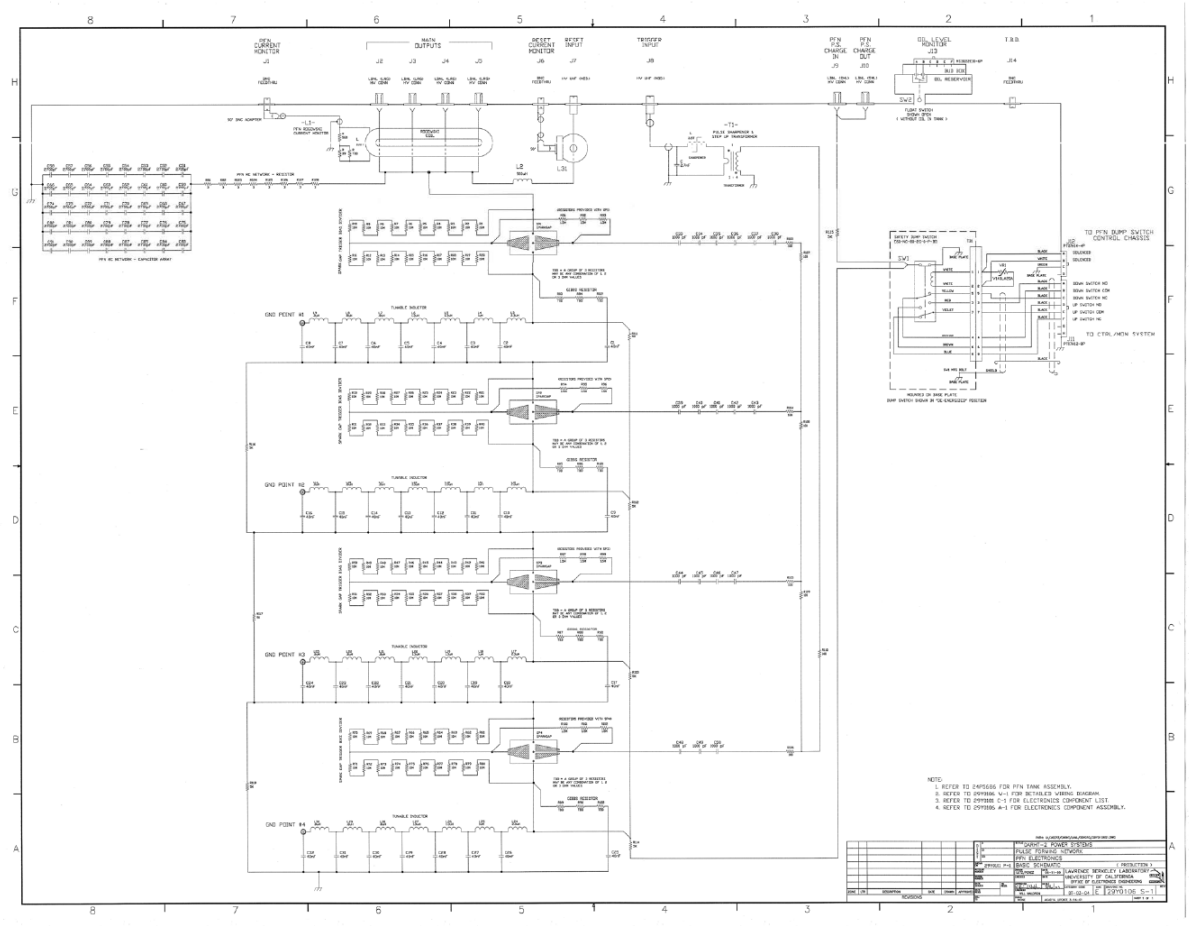

FIGURE 5: CIRCUIT DESIGN OF DARHT PFN

The circuit drawing was then adapted into an LTSpice file. Here is the layout of the simulated circuitry:

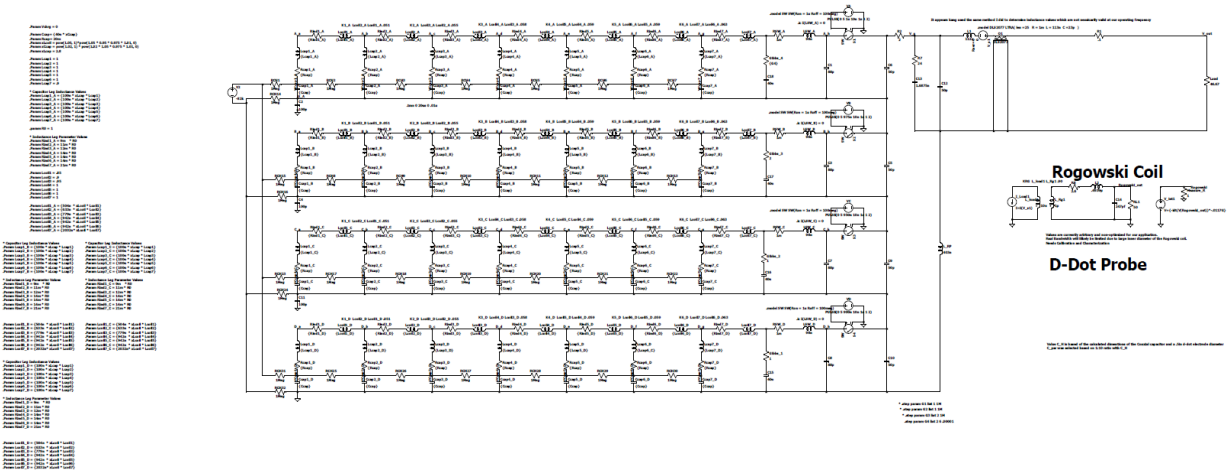

FIGURE 6: LTSPICE CIRCUIT SIMULATION OF DARHT PFN WITH STEPPED GIBBS RESISTOR VALUES IMPLEMENTED

Each horizontal stage stacked with capacitor-resistor-inductor meshes forms a single MARX stage. As can be seen in the drawing, there are four stages. The current travels from the bottom up, meaning the fourth stage is the final stage of the MARX. The fourth-stage Gibbs resistor is built into the righthand side of the stage circuitry.

The load is modelled in Figure 6, and the Rogowski coil has been modeled just to the bottom of the load. Running LTSpice provides information on how the waveforms of the PFN should look once fired. The output of the current read by the simulated Rogowski coil can be extracted and plotted in MATLAB, as was done for this test. The charge voltage used to simulate the current waveforms was 60kV, as this is the testing voltage used on the PFNs. The fourth-stage Gibbs resistor was first modelled using a baseline value of 2 Ω. The simulation was then run using a Gibbs resistor with an established resistance of 6 Ω and 0 Ω. The following waveforms were produced running this simulation:

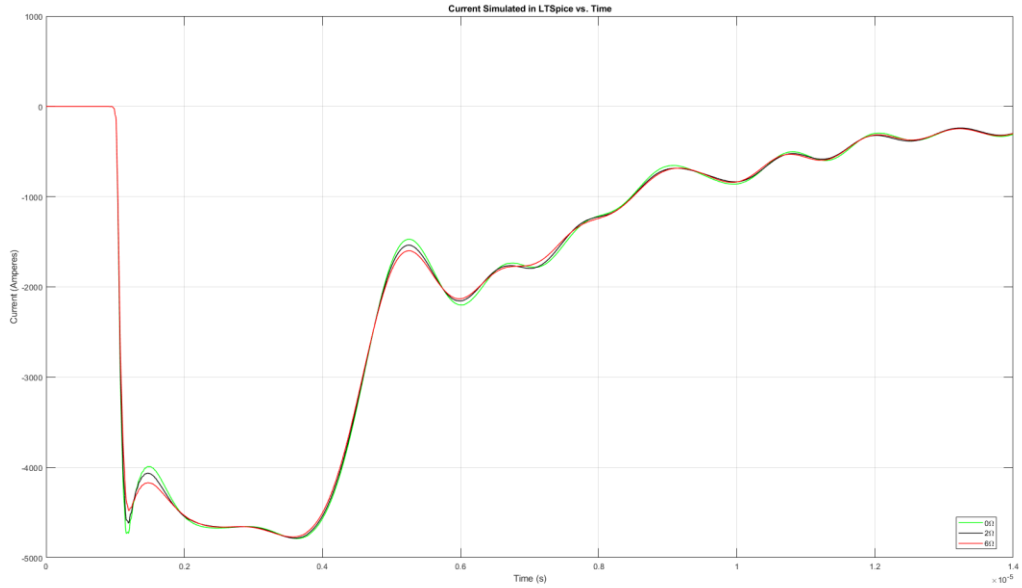

FIGURE 7: PFN CURRENT SIMULATED IN LTSPICE WITH STEPPED FOURTH-STAGE GIBBS RESISTOR VALUES

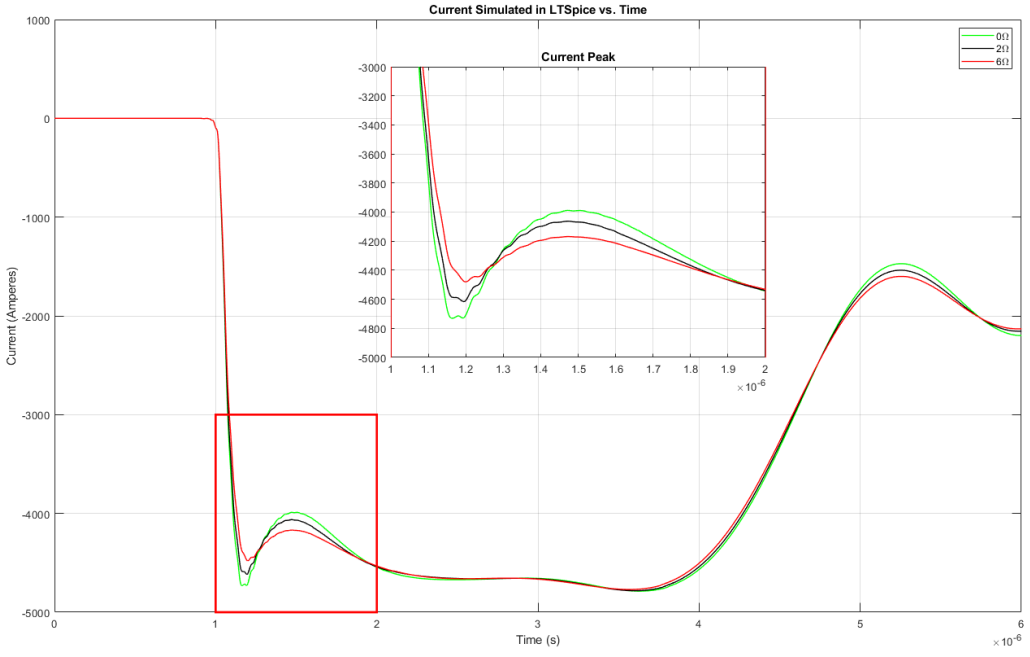

FIGURE 8: ENLARGED VIEW OF FIRST CURRENT PEAK APPEARING IN PFN SIGNAL (SIMULATED IN LTSPICE)

There is a prominent peak appearing at the left-hand side of the waveform that is sharpened or dulled by the value of the resistance of the Gibbs resistor. As expected, the current peak rounds

out (or decreases) as the resistance increases, and the peak sharpens (or increases) as the resistance decreases. This trend is what is to be expected from extracted waveforms provided by the test stand data.

Indeed, in comparing the simulated current waveforms to the output currents provided by the test stand data, the trend holds. The following figures provide information on the behavior of the PFN current when the value of the Gibbs' resistance is altered.

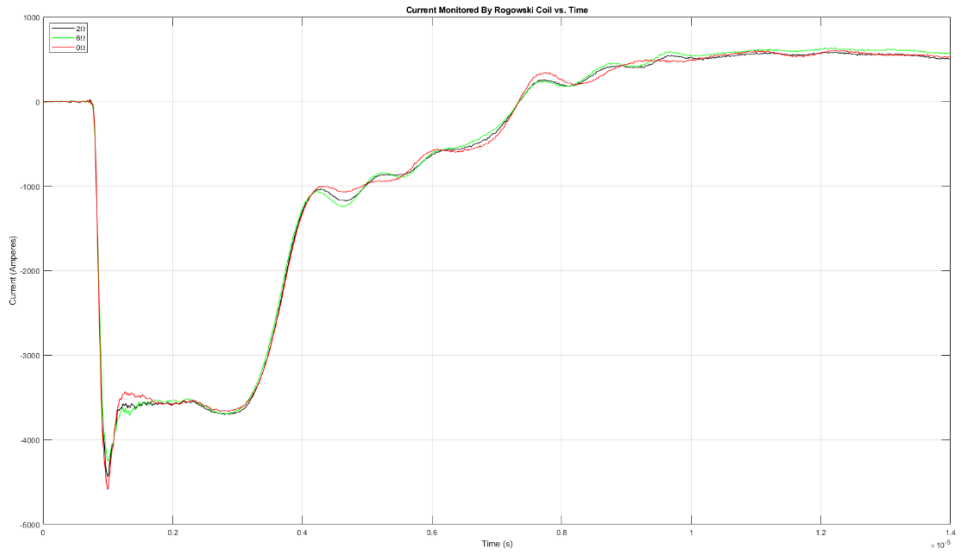

FIGURE 9: OUTPUT CURRENT OF TEST STAND PFN MONITORED BY ROGOWSKI COIL

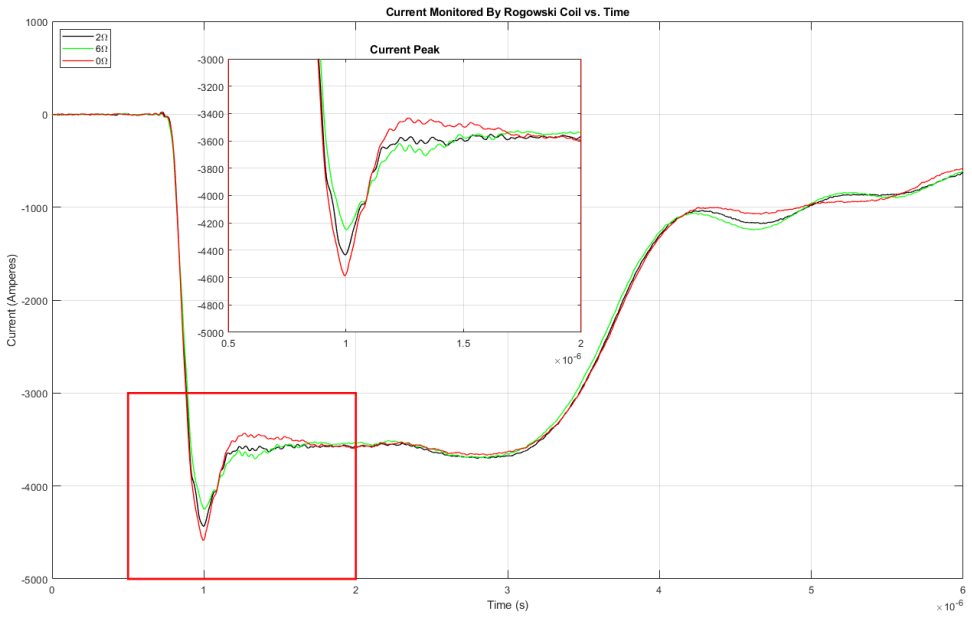

FIGURE 10: VIEW OF FIRST CURRENT SPIKE IN PFN SIGNAL, MONITORED BY ROGOWSKI COIL

The trend of the experimental waveforms matches that of the simulated waveforms. As the Gibbs resistance was increased, the current peak decreased, and as the Gibbs resistance decreased, the current peak increased. The following images provide a visual interpretation of the differences between the baseline signal and the two altered resistances:

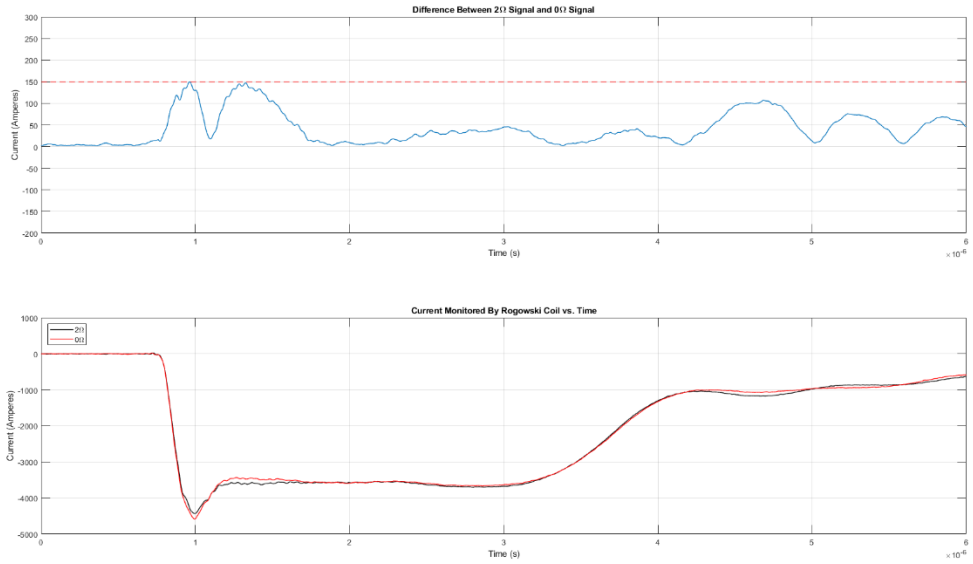

FIGURE 11: DIFFERENCE BETWEEN TEST STAND DATA PROVIDED BY 2 OHM RESISTOR AND 0 OHM RESISTOR (MARKER AT DIFFERENCE BETWEEN THE FIRST PEAKS OF BOTH SIGNALS)

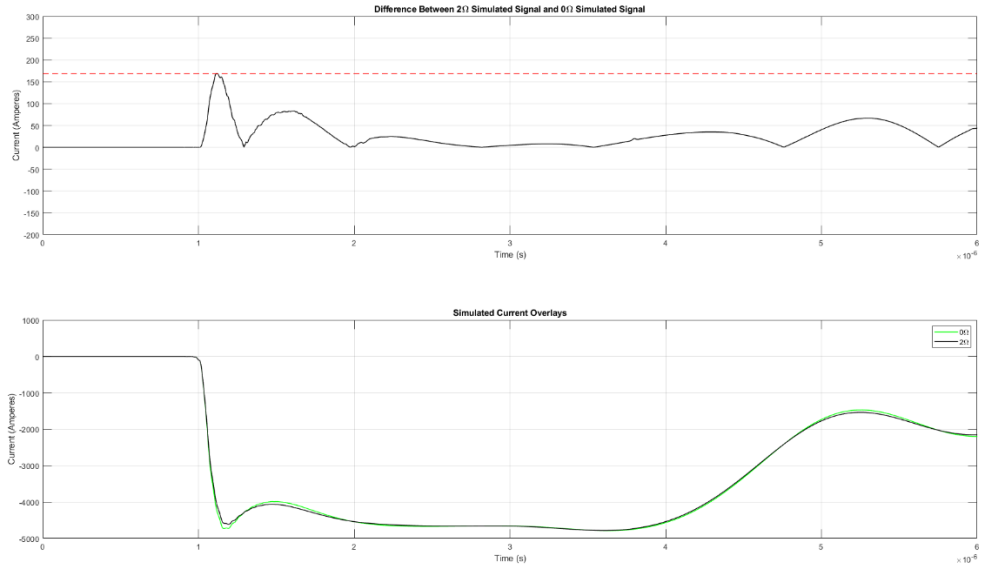

FIGURE 12: DIFFERENCE BETWEEN SIMULATED LTSPICE DATA PROVIDED BY 2 OHM RESISTOR AND 0 OHM RESISTOR (MARKER AT DIFFERENCE BETWEEN THE FIRST PEAKS OF BOTH SIGNALS)

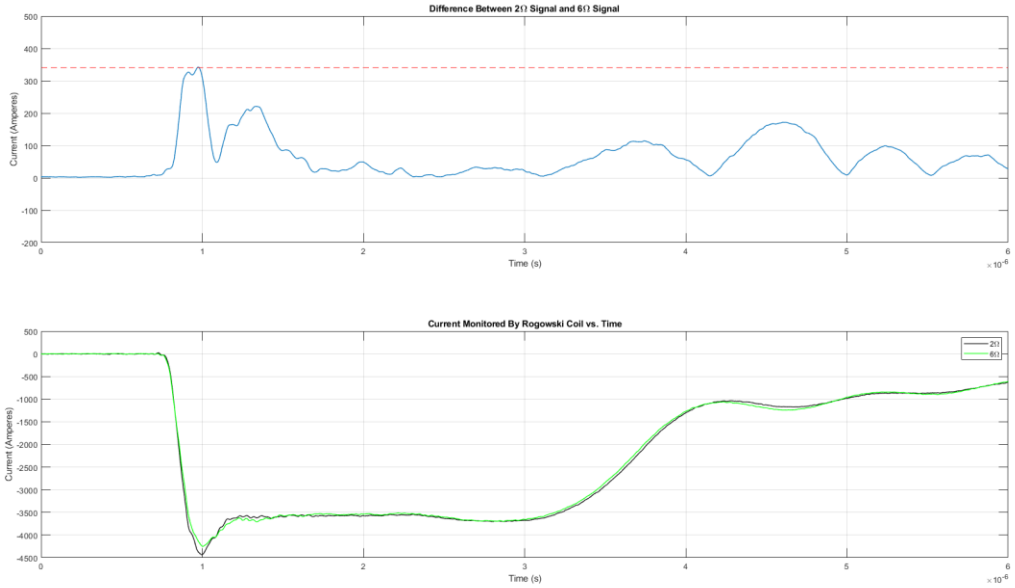

FIGURE 13: DIFFERENCE BETWEEN TEST STAND DATA PROVIDED BY 2 OHM RESISTOR AND 6 OHM RESISTOR (MARKER AT DIFFERENCE BETWEEN THE FIRST PEAKS OF BOTH SIGNALS)

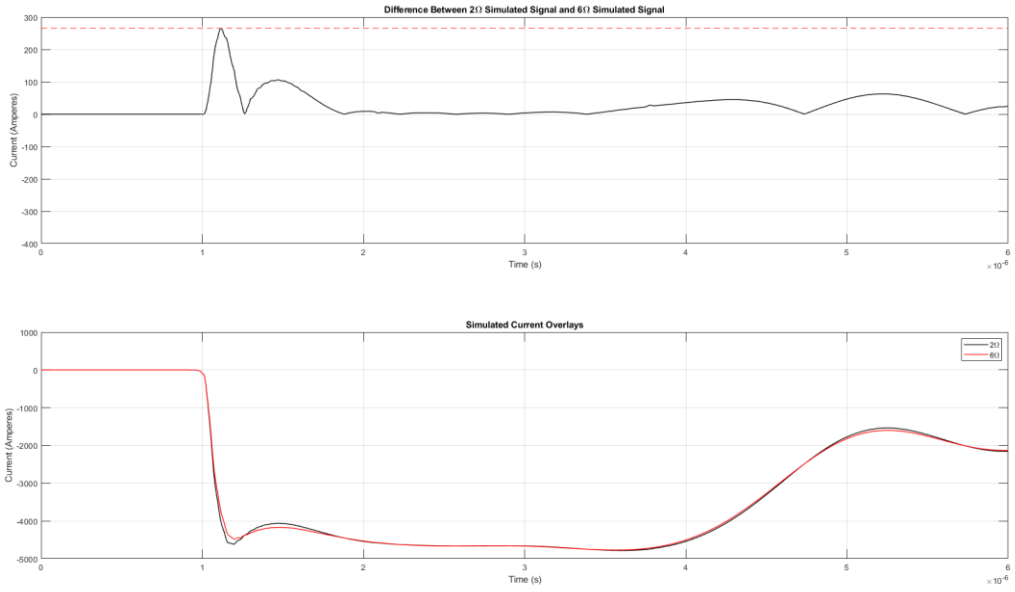

FIGURE 14: DIFFERENCE BETWEEN SIMULATED LTSPICE DATA PROVIDED BY 2 OHM RESISTOR AND 6 OHM RESISTOR (MARKER AT DIFFERENCE BETWEEN THE FIRST PEAKS OF BOTH SIGNALS)

As can be seen in Figures 11 through 14**,** the height of the sharp peak at the beginning of the current waveform is directly affected by any alterations made to the value of the resistance of the

fourth-stage Gibbs Resistor. The 150kA to 300kA resistance difference is visible to the naked eye, a dip or spike in current that can be spotted by an observer actively monitoring pulse shots.

10.2 DARHT Waveforms

Data was collected from the DARHT database so that it might be compared to waveforms provided by the test stand set-up. Shot data was collected from the database corresponding to a shot day when the fourth-stage Gibbs resistor was known to have failed. All PFN current waveforms were collected from shots leading up to the complete failure of the Gibbs. The following image is of said waveforms:

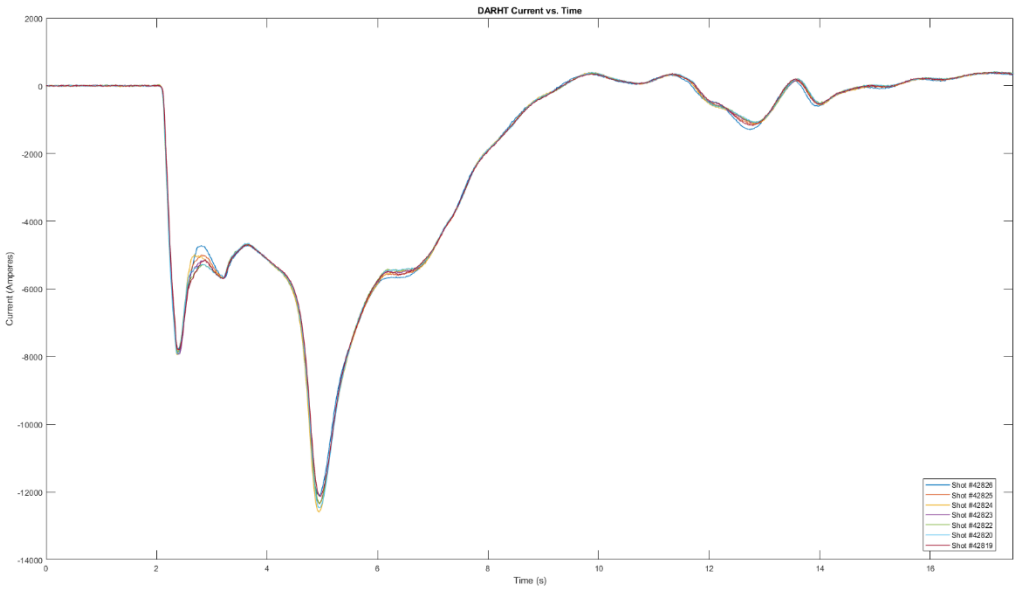

FIGURE 15: DARHT CURRENT WAVEFORMS, TAKEN DURING A SHOT DAY WHEN THE FOURTH-STAGE GIBBS RESISTOR FAILED

The shot numbers appearing in the legend are sequential. For the most part the waveforms followed the expected trend: that is, as the Gibbs resistor began to break, the current was dampened. This is indicative of an increasing resistance of the Gibbs. The difference between one of the first beam-loaded shots taken that day and one of the last beam-loaded shots is as follows:

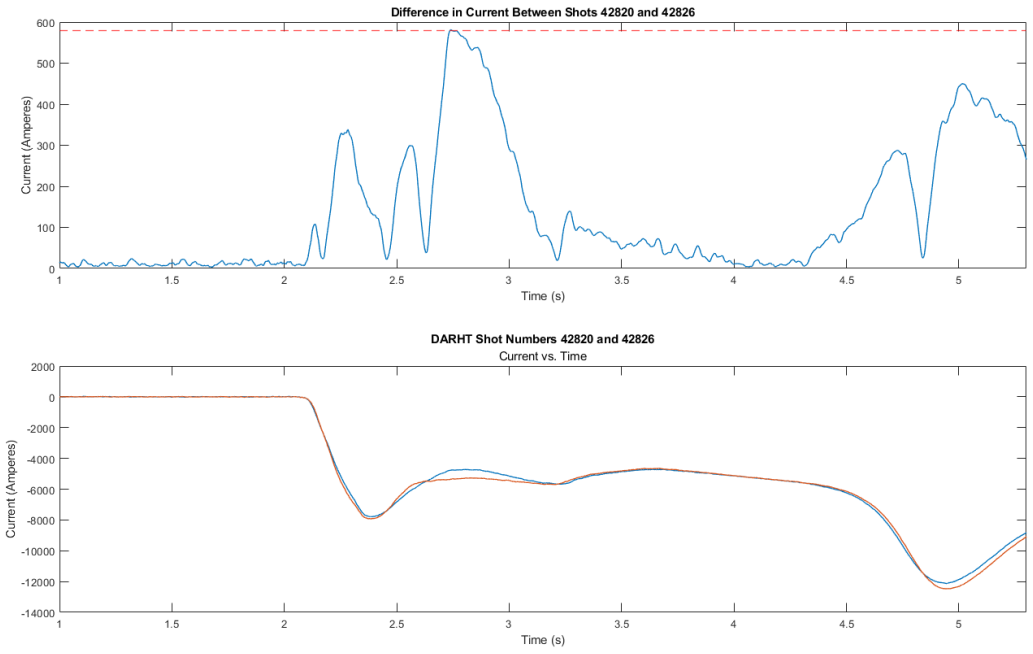

FIGURE 16: DIFFERENCE BETWEEN SHOT TAKEN EARLY IN THE DAY VS SHOT TAKEN LATER IN THE DAY, WITH MARKER PLACED AT LARGEST DIFFERENCE BETWEEN THE TWO SIGNALS

The tallest peak plotted in Figure 16 signifies the largest differences in current amplitude that can be visibly spotted by an operator. The maximum difference between the Gibbs' resistance in a healthy state and a failing Gibbs is roughly 580kA, an even larger difference than that provided by the test data. As these current waveforms appear before an operator after each accelerator shot, this difference in current can be caught, if indicators are properly implemented.

11 Proposed Implementation of the SHM System

During operation of the accelerator, current waveforms provided by the Rogowski coils built into the PFNs are logged to the database after each shot. Unfortunately, the waveforms belonging to each PFN do not automatically appear on screen, as there are sixty-six PFNs driving the beam through the accelerator. One would need to sift through the current readouts of each PFN after every accelerator shot. In addition to this, the waveforms are not automatically overlayed over waveforms belonging to previous shots, so the data is not brought up atop a standard of comparison unless the operator manually overlays all shot data taken throughout the day. To do this for each PFN would be cumbersome and would take hours.

The proposed solution to this issue is to work an alert system into the software being used to read out current waveforms. That is, to set a tolerance zone around the timeframe that the current spike is known to appear. It is important that a tolerance zone is established, and *not* a set current value, as the current spike value of each PFN differs from its neighbor. Ergo, there should be a minimum and maximum deviation established around the baseline current produced by the PFN. Then, if the signal deviates from its standard current output, an operator can be notified by the

system, and they'll know to check the waveforms of the PFN with the deviating current. If the current dips below the threshold, one may conclude that the fourth-stage Gibbs resistor is actively failing. If the current exceeds the threshold, then one may conclude that the Gibbs resistor is completely damaged.

As a standard of comparison, to understand how little the current signal should be deviating from itself over the course of several shots a day, the following was data collected from an undamaged PFN:

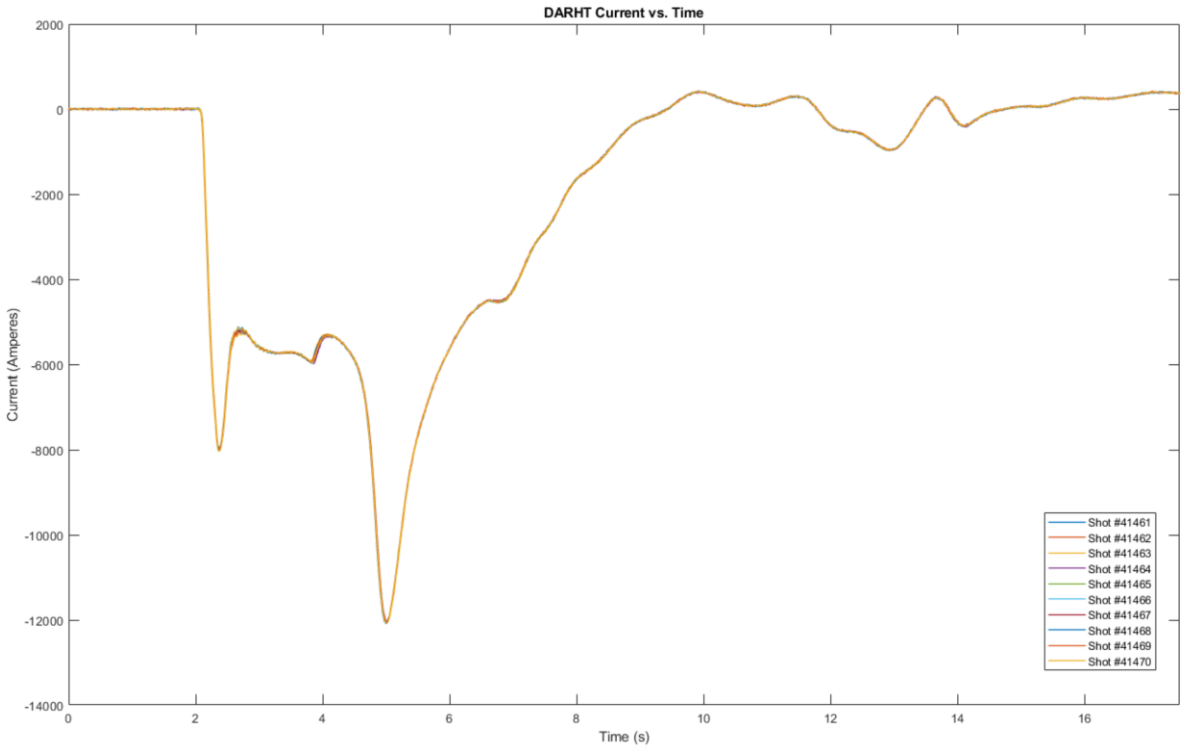

FIGURE 17: UNDAMAGED PFN CURRENT SIGNAL

There is very little deviation in the Figure 17 waveforms. Furthermore, these current signals are provided by the same PFN that underwent refurbishment for a broken Gibbs resistor. The data extracted from this PFN's database established results relaying information about the broken Gibbs (i.e. this is the data belonging to the earlier PFN before it broke).

Once an operator has been alerted to the potential damage, it will be up to them to decide whether they'd like to take a few more shots to confirm the presence of a failing or failed Gibbs resistor, or if they'd like to remove the PFN from the axis hall. The former decision will be made with the understanding that confirming the diagnostic is working comes with the price of potentially destroying a failing resistor; or sending current through an oil gap, meaning circuit components may be destroyed. The latter decision is accompanied by the knowledge that the change in current peaks could be an anomaly and the operator's call was too safe. However, if a failing resistor can be caught and replaced (verses a *failed* resistor), then time spent replacing a potentially healthy Gibbs is made up by assuring time is *not* spent checking the PFN for additional broken circuit components.

12 Experimental Errors

A few experimental errors were taken note of over the duration of this test. The first issue that arose was the difference between the simulated LTSpice waveforms and the test stand waveforms. This discrepancy may arise from the fact that the induction values allotted to the inductors created in the simulation may not be valid at the DARHT operating frequency. This issue could be solved by taking measurements of inductance values of each inductor built into the four MARX stages. The scope of the project was short, with five weeks of time allotted to data collection. It could not have been known that the induction values of the test stand's inductors don't match those of the simulated induction values until *after* the test stand data was analyzed, at which point it was too late to gather information on the induction values. Therefore, before proceeding in enacting future tests, the LTSpice model needs to be altered accordingly.

Another issue that may be noted in the experimental data is that the resistance load used during the test stand experiment does not match that of the PFN load at DARHT. The load at DARHT is an induction cell, a difficult load to simulate. The load used at the test stand was not built to match the load at DARHT, and the simulation designed in LTSpice followed the test stand schematic. This means that both simulated waveforms and test stand waveforms do not match those of DARHT's. The current waveforms produced by DARHT PFNs have a large dip within the pulse, forcing the square wave to peak sharply around the edges. This is a sharp contrast to the rectangular wave produced by the test stand load. However, for this experiment, it was not the shape of the output current that mattered so much as the behavior. The key feature being measured was the difference between the baseline waveform and the waveforms produced by PFNs built using 6 Ω Gibbs resistors and a short. Ergo, the experimental data is still valuable, as it shows the change in the first peak found at the edge of both DARHT current waveforms and current waveforms provided by the test stand. The proposed solution would require a redesign of the test load circuit, a project that would require input from an electrical engineer.

Another issue that arose during data collection was the inconsistencies in DARHT waveforms. Unfortunately, there were a limited number of days that data could be pulled from for purposes of this experiment. In checking the logbooks, there were only three PFNs pulled due to the failure of a fourth-stage Gibbs resistor. Two out of the three of these data sets provided promising data: that is, waveforms that fluctuated during shots running up to failure. This signifies that the other data set was pulled from days when the Gibbs may not have been actively failing, or that the active failure of the Gibbs may not offer a significant enough change to affect the current waveforms. However, neither conclusion can be reached, as one source of data did provide altered waveforms as the Gibbs (presumably) failed. These waveforms didn't follow a specific trend between shot-to-shot during failure (i.e. while the waveform belonging to the first shot number had a higher peak than the last shot number, the shots in between fluctuated in height in a nonlinear manner); but this does not negate the fact that the overall trend showed a dip in the current's peak. The proposed solution to this issue is to collect test data from PFNs with purposefully broken Gibbs resistors installed in the fourth stage.

The last issue encountered whilst running the experiment was less a design flaw and more so a timing error. Information on how the PFN waveform would look with an oil gap is integral to

pinpointing a PFN with a Gibbs resistor that has failed. This test will be finished out in due course, and final results will be updated accordingly.

13 Conclusion

Axis II of DARHT is reliant on the PFNs to keep the induction cells running properly. If a PFN breaks, all work must be paused to replace the broken PFN. Spare PFNs are essential, and anything that can be done to reduce the time it takes to refurbish a PFN that has failed is beneficial to both the technicians who must repair the PFNs and the accelerator operators who must maintain a tight shot schedule. Monitoring the fourth-stage Gibbs resistor would benefit both parties, as the PFN refurbishment team would not need to use extra time to check for busted circuit components when replacing the fourth-stage Gibbs, and operators could rest assured that spare PFNs would be made available anytime a new issue arises with the PFNs.

The key benefit to the proposed SHM system is the fact that no new structure or system design would need to be implemented. The diagnostic tool, the Rogowski coil, is already built into the system. If implemented, all that would need to be done is a slight alteration to the code used to read out the PFN current waveforms. A tolerance threshold would surround the first peak of the output current, and an operator would be alerted to a breaching of this threshold. The diagnostic is simple, but it could save the PFN refurbishment team time when they change out the failing Gibbs resistor, as they would not have to allocate extra time to checking for additional broken components in the PFN.

Ultimately, the proposed SHM system is safe, easy to implement, and cost-effective. While more tests need to be run before implementation can be approved, the system is promising.

14 Works Cited

Cook, Edward G., and Eikki Hotta. “4.1 General Discussion on Induction Accelerator Modulators.” *Induction Accelerators*, Springer, London, 2011, pp. 39–58.

Jill Gibson. “The Dual-Axis Radiographic Hydrodynamic Test Facility.” *Jill Gibson*, 20 Mar. 2025, www.lanl.gov/media/publications/national-security-science/0423-the-dual-axis-radiographic-hydrodynamic-test-facility.

Los Alamos National Laboratory. “DARHT Facility.” *Los Alamos National Laboratory*, www.lanl.gov/science-engineering/science-facilities/darht. Accessed 21 May 2025.

Los Alamos Reporter. “Newly-Completed Weather Enclosure at LANL DARHT Facility Expected to Increase Productivity by 43 Percent.” *Los Alamos Reporter*, 17 July 2020, losalamosreporter.com/2020/07/17/newly-completed-weather-enclosure-at-darht-expected-to-increase-productivity-by-43-percent/.

“Pulse Forming Networks.” *General Atomics*, www.ga.com/capacitors/pulse-forming-networks. Accessed 21 May 2025.

“Resistors for Power Electronics.” *High Energy Disk*, HVR Advanced Power Components, 2005, www.hvrapc.com/highenergydisk.asp.

Waldron, W.L., and L.L. Reginato. “Design and performance of the DARHT second axis induction cells and drivers.” *Conference Record of the 2000 Twenty-Fourth International Power Modulator Symposium*, 2000, pp. 179–182, https://doi.org/10.1109/modsym.2000.896194.

“The Rogowski Coil.” *PEM UK*, www.pemuk.com/support/the-rogowski-coil. Accessed 21 May 2025.